

Detrended partial cross-correlation analysis of two nonstationary time series influenced by common external forces

Xi-Yuan Qian,^{1,2} Ya-Min Liu,¹ Zhi-Qiang Jiang,^{2,3} Boris Podobnik,^{4,5,6,7} Wei-Xing Zhou,^{1,2,3,*} and H. Eugene Stanley^{4,†}

¹*School of Science, East China University of Science and Technology, Shanghai 200237, China*

²*Research Center for Econophysics, East China University of Science and Technology, Shanghai 200237, China*

³*School of Business, East China University of Science and Technology, Shanghai 200237, China*

⁴*Center for Polymer Studies and Department of Physics, Boston University, Boston, MA 02215, USA*

⁵*Faculty of Civil Engineering, University of Rijeka, 51000 Rijeka, Croatia*

⁶*Zagreb School of Economics and Management, 10000 Zagreb, Croatia*

⁷*Faculty of Economics, University of Ljubljana, 1000 Ljubljana, Slovenia*

(Dated: January 28, 2022)

When common factors strongly influence two power-law cross-correlated time series recorded in complex natural or social systems, using classic detrended cross-correlation analysis (DCCA) without considering these common factors will bias the results. We use detrended partial cross-correlation analysis (DPXA) to uncover the intrinsic power-law cross-correlations between two simultaneously recorded time series in the presence of nonstationarity after removing the effects of other time series acting as common forces. The DPXA method is a generalization of the detrended cross-correlation analysis that takes into account partial correlation analysis. We demonstrate the method by using bivariate fractional Brownian motions contaminated with a fractional Brownian motion. We find that the DPXA is able to recover the analytical cross Hurst indices, and thus the multi-scale DPXA coefficients are a viable alternative to the conventional cross-correlation coefficient. We demonstrate the advantage of the DPXA coefficients over the DCCA coefficients by analyzing contaminated bivariate fractional Brownian motions. We calculate the DPXA coefficients and use them to extract the intrinsic cross-correlation between crude oil and gold futures by taking into consideration the impact of the US dollar index. We develop the multifractal DPXA (MF-DPXA) method in order to generalize the DPXA method and investigate multifractal time series. We analyze multifractal binomial measures masked with strong white noises and find that the MF-DPXA method quantifies the hidden multifractal nature while the MF-DCCA method fails.

PACS numbers: 89.75.Da, 05.45.Tp, 05.45.Df, 05.40.-a

I. INTRODUCTION

Complex systems with interacting constituents are ubiquitous in nature and society. To understand the microscopic mechanisms of emerging statistical laws of complex systems, one records and analyzes time series of observable quantities. These time series are usually nonstationary and possess long-range power-law cross-correlations. Examples include the velocity, temperature, and concentration fields of turbulent flows embedded in the same space as joint multifractal measures [1, 2], topographic indices and crop yield in agronomy [3, 4], temporal and spatial seismic data [5], nitrogen dioxide and ground-level ozone [6], heart rate variability and brain activity in healthy humans [7], sunspot numbers and river flow fluctuations [8], wind patterns and land surface air temperatures [9], traffic flows [10] and traffic signals [11], self-affine time series of taxi accidents [12], and econophysical variables [13–17].

A variety of methods have been used to investigate the long-range power-law cross-correlations between two

nonstationary time series. The earliest was joint multifractal analysis to study the cross-multifractal nature of two joint multifractal measures through the scaling behaviors of the joint moments [1, 2, 18–20], which is a multifractal cross-correlation analysis based on the partition function approach (MF-X-PF) [21]. Over the past decade, detrended cross-correlation analysis (DCCA) has become the most popular method of investigating the long-range power-law cross correlations between two nonstationary time series [14, 22–24], and this method has numerous variants [25–33]. Statistical tests can be used to measure these cross correlations [34–36]. There is also a group of multifractal detrended fluctuation analysis (MF-DCCA) methods of analyzing multifractal time series, e.g., MF-X-DFA [37], MF-X-DMA [38], and MF-HXA [39].

The observed long-range power-law cross-correlations between two time series may not be caused by their intrinsic relationship but by a common third driving force or by common external factors [40–42]. If the influence of the common external factors on the two time series are additive, we can use partial correlation to measure their intrinsic relationship [43]. To extract the intrinsic long-range power-law cross-correlations between two time series affected by common driving forces, we previously developed and used detrended partial cross-

* wxzhou@ecust.edu.cn

† hes@bu.edu

correlation analysis (DPXA) and studied the DPXA exponents of variable cases, combining the ideas of detrended cross-correlation analysis and partial correlation [44]. In Ref. [45], the DPXA method has been proposed independently, focussing on the DPXA coefficient.

Here we provide a general framework for the DPXA and MF-DPXA methods that is applicable to various extensions, including different detrending approaches and higher dimensions. We adopt two well-established mathematical models (bivariate fractional Brownian motions and multifractal binomial measures) in our numerical experiments, which have known analytical expressions, and demonstrate how the (MF-)DPXA methods is superior to the corresponding (MF-)DCCA methods.

II. DETRENDED PARTIAL CROSS-CORRELATION ANALYSIS

A. DPXA exponent

Consider two stationary time series $\{x(t) : t = 1, \dots, T\}$ and $\{y(t) : t = 1, \dots, T\}$ that depend on a sequence of time series $\{z_i(t) : t = 1, 2, \dots, T\}$ with $i = 1, \dots, n$. Each time series is covered with $M_s = \lceil T/s \rceil$ non-overlapping windows of size s . Consider the v th box $[l_v + 1, l_v + s]$, where $l_v = (v - 1)s$. We calibrate the two linear regression models for \mathbf{x}_v and \mathbf{y}_v respectively,

$$\begin{cases} \mathbf{x}_v = \mathbf{Z}_v \boldsymbol{\beta}_{x,v} + \mathbf{r}_{x,v} \\ \mathbf{y}_v = \mathbf{Z}_v \boldsymbol{\beta}_{y,v} + \mathbf{r}_{y,v} \end{cases}, \quad (1)$$

where $\mathbf{x}_v = [x_{l_v+1}, \dots, x_{l_v+s}]^T$, $\mathbf{y}_v = [y_{l_v+1}, \dots, y_{l_v+s}]^T$, $\mathbf{r}_{x,v}$ and $\mathbf{r}_{y,v}$ are the vectors of the error term, and

$$\mathbf{Z}_v = \begin{pmatrix} \mathbf{z}_{v,1}^T \\ \vdots \\ \mathbf{z}_{v,p}^T \end{pmatrix} = \begin{pmatrix} z_1(l_v + 1) & \cdots & z_p(l_v + 1) \\ \vdots & \ddots & \vdots \\ z_1(l_v + s) & \cdots & z_p(l_v + s) \end{pmatrix} \quad (2)$$

is the matrix of the p external forces in the v th box, where \mathbf{x}^T is the transform of \mathbf{x} . Equation (1) gives the estimates $\hat{\boldsymbol{\beta}}_{x,v}$ and $\hat{\boldsymbol{\beta}}_{y,v}$ of the p -dimensional parameter vectors $\boldsymbol{\beta}_{x,v}$ and $\boldsymbol{\beta}_{y,v}$ and the sequence of error terms,

$$\begin{cases} \mathbf{r}_{x,v} = \mathbf{x}_v - \mathbf{Z}_v \hat{\boldsymbol{\beta}}_{x,v} \\ \mathbf{r}_{y,v} = \mathbf{y}_v - \mathbf{Z}_v \hat{\boldsymbol{\beta}}_{y,v} \end{cases}. \quad (3)$$

We obtain the disturbance profiles, i.e.,

$$\begin{cases} R_{x,v}(k) = \sum_{j=1}^k r_x(l_v + j) \\ R_{y,v}(k) = \sum_{j=1}^k r_y(l_v + j) \end{cases}, \quad (4)$$

where $k = 1, \dots, s$.

We assume that the local trend functions of $R_{x,v}$ and $R_{y,v}$ are $\tilde{R}_{x,v}$ and $\tilde{R}_{y,v}$, respectively. The detrended partial cross-correlation in each window is then calculated,

$$F_v^2(s) = \frac{1}{s} \sum_{k=1}^s [R_{x,v}(k) - \tilde{R}_{x,v}(k)] [R_{y,v}(k) - \tilde{R}_{y,v}(k)], \quad (5)$$

and the second-order detrended partial cross-correlation is calculated,

$$F_{xy;z}(2, s) = \left[\frac{1}{m-1} \sum_{v=1}^m F_v^2(s) \right]^{1/2}. \quad (6)$$

If there are intrinsic long-range power-law cross-correlations between x and y , we expect the scaling relation,

$$F_{xy;z}(2, s) \sim s^{h_{xy;z}}. \quad (7)$$

There are many ways of determining $\tilde{R}_{x,v}$ and $\tilde{R}_{y,v}$. The local detrending functions could be polynomials [46, 47], moving averages [48–51], or other possibilities [52]. To distinguish the different detrending methods, we label the corresponding DPXA variants as, e.g., PX-DFA and PX-DMA. When the moving average is used as the local detrending function, the window size of the moving averages must be the same as the covering window size s [53].

To measure the validity of the DPXA method, we perform numerical experiments using an additive model for x and y , i.e.,

$$\begin{cases} x(t) = \beta_{x,0} + \beta_x z(t) + r_x(t) \\ y(t) = \beta_{y,0} + \beta_y z(t) + r_y(t) \end{cases}, \quad (8)$$

where $z(t)$ is a fractional Gaussian noise with Hurst index H_z , and r_x and r_y are the incremental series of the two components of a bivariate fractional Brownian motion (BFBMs) with Hurst indices H_{r_x} and H_{r_y} [54–56]. The properties of multivariate fractional Brownian motions have been extensively studied [54–56]. In particular, it has been proven that the Hurst index $H_{r_x r_y}$ of the cross-correlation between the two components is [54–56]

$$H_{r_x r_y} = (H_{r_x} + H_{r_y})/2. \quad (9)$$

This property allows us to assess how the proposed method perform. We can obtain the h_{xy} of x and y using the DCCA method and the $h_{xy;z}$ of r_x and r_y using the DPXA method. Our numerical experiments show that $H_{r_x r_y} = h_{r_x r_y} = h_{xy;z} \neq h_{xy}$. We use H for theoretical or true values and h for numerical estimates.

In the simulations we set $\beta_{x,0} = 2$, $\beta_x = 3$, $\beta_{y,0} = 2$, and $\beta_y = 3$ in the model based on Eq. (8). Three Hurst indices H_{r_x} , H_{r_y} , and H_z are input arguments and vary from 0.1 to 0.95 at 0.05 intervals. Because r_x and r_y are symmetric, we set $H_{r_x} \leq H_{r_y}$, resulting in $\frac{(18+1) \times 18}{2} \times 18 = 3078$ triplets of (H_{r_x}, H_{r_y}, H_z) . The BFBMs are simulated using the method described in Ref. [55, 56], and the FBMs are generated using a rapid wavelet-based approach [57]. The length of each time series is 65536. For each (H_{r_x}, H_{r_y}, H_z) triplet we conduct 100 simulations. We obtain the Hurst indices for the simulated time series r_x , r_y , z , x , and y using detrended fluctuation analysis [46, 58]. The average values

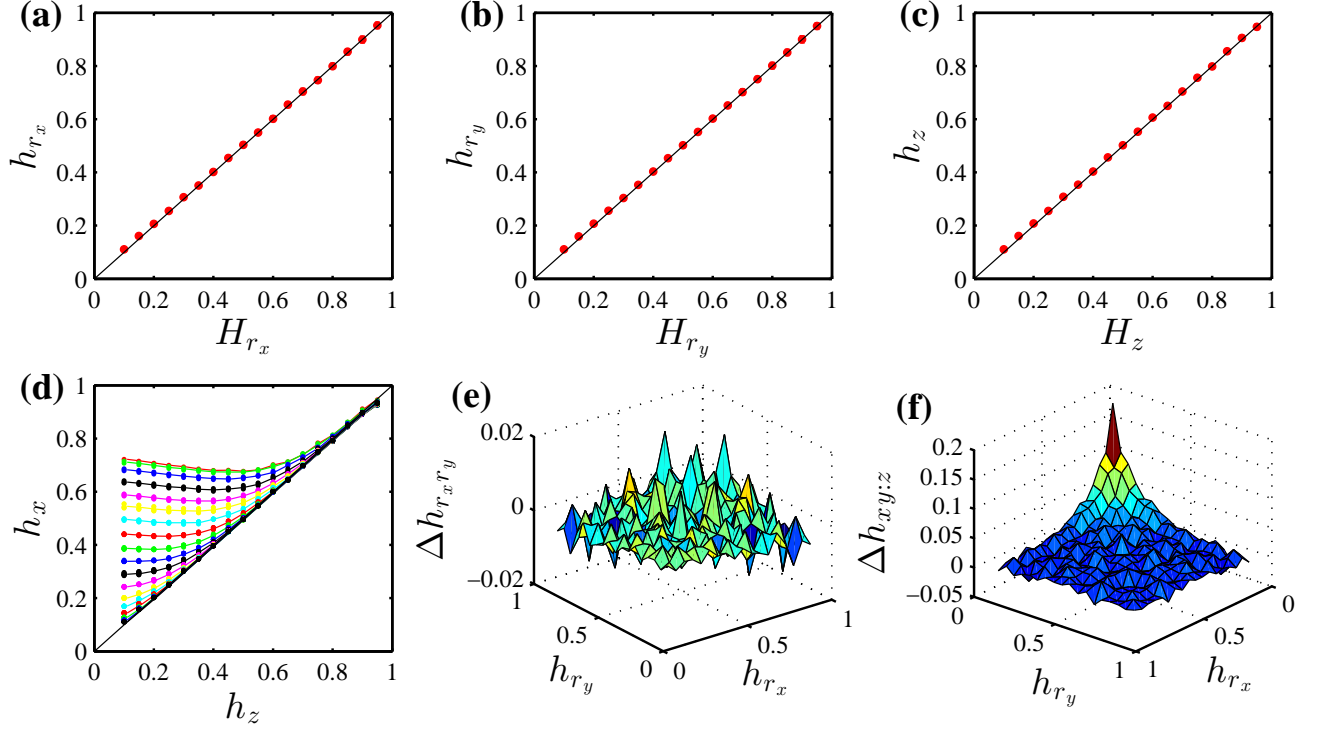


FIG. 1. (color online.) Detrended partial cross-correlation exponents. (a-b) Dependence of the average Hurst indices h_{r_x} and h_{r_y} of the two components of the generated bivariate fractional Brownian motions on the input Hurst indices H_{r_x} and H_{r_y} . (c) Dependence of the average Hurst index h_z of the generated univariate fractional Brownian motions on the input Hurst index H_z . (d) Dependence of h_x on H_z for different h_{r_x} values. (e) Relative error $\Delta h_{r_x r_y} = h_{r_x r_y} - H_{r_x r_y}$. (f) Relative error $\Delta h_{xy:z}$ between the DPXA estimate $\langle h_{xy:z} \rangle_z$ and the true value $h_{r_x r_y}$ as a function of h_{r_x} and h_{r_y} .

h_{r_x} , h_{r_y} , h_z , h_x , and h_y over 100 realizations are calculated for further analysis, which are shown in Fig. 1. A linear regression between the output and input Hurst indices in Fig. 1(a-c) yields $\langle h_{r_x} \rangle = 0.009 + 0.990H_{r_x}$, $\langle h_{r_y} \rangle = 0.009 + 0.990H_{r_y}$, and $\langle h_z \rangle = 0.010 + 0.991H_z$, suggesting that the generated FBMs have Hurst indices equal to the input Hurst indices. Figure 1(d) shows that when $h_{r_x} \leq h_z$, h_x is close to h_z . When it is not, $h_z < h_x < h_{r_x}$.

Figure 1(e) shows that $h_{r_x r_y} = (h_{r_x} + h_{r_y})/2$. Because $h_{r_x} \approx H_{r_x}$ and $h_{r_y} \approx H_{r_y}$ [see Fig. 1(a)-(b)], we verify numerically that

$$h_{r_x r_y} \approx H_{r_x r_y}. \quad (10)$$

Note also that $h_{xy} \approx (h_x + h_y)/2$, and that $h_{xy:z}$ is a function of h_{r_x} , h_{r_y} and h_z . A simple linear regression gives

$$h_{xy:z} = 0.003 + 0.509h_{r_x} + 0.493h_{r_y} + 0.012h_z, \quad (11)$$

which indicates that the DPXA method can be used to extract the intrinsic cross-correlations between the two time series x and y when they are influenced by a common factor z . We calculate the average $\langle h_{xy:z} \rangle_z$ over different H_z and then find the relative error

$$\Delta h_{xy:z} = \frac{\langle h_{xy:z} \rangle_z - h_{r_x r_y}}{h_{r_x r_y}}. \quad (12)$$

Figure 1(f) shows the results for different combinations of h_{r_x} and h_{r_y} . Although in most cases we see that $\Delta h_{xy:z} \ll 0.05$, when both h_{r_x} and h_{r_y} approach 0, $\Delta h_{xy:z}$ increases. When $h_{r_x} = h_{r_y} = 0.11$, $\Delta h_{xy:z} = 0.192$, and when $h_{r_x} = 0.11$ and $h_{r_y} = 0.16$, $\Delta h_{xy:z} = 0.113$. For all other points of (h_{r_x}, h_{r_y}) , the relative errors $\Delta h_{xy:z}$ are less than 0.10.

B. DPXA coefficient

In a way similar to detrended cross-correlation coefficients [31, 35], we define the detrended partial cross-correlation coefficient (or DPXA coefficient) as

$$\rho_{\text{DPXA}}(s) = \rho_{xy:z}(s) = \frac{F_{xy:z}^2(2, s)}{F_{x:z}(2, s)F_{y:z}(2, s)}. \quad (13)$$

As in the DCCA coefficient [31, 36], we also find $-1 \leq \rho_{\text{DPXA}}(s) \leq 1$ for DPXA. The DPXA coefficient indicates the intrinsic cross-correlations between two non-stationary series.

We use the mathematical model in Eq. (8) with the coefficients $\beta_{x,0} = \beta_{y,0} = 2$ and $\beta_{x,1} = \beta_{y,1} = 3$ to demonstrate how the DPXA coefficient outperforms the DCCA coefficient. The two components r_x and r_y of the BFBM

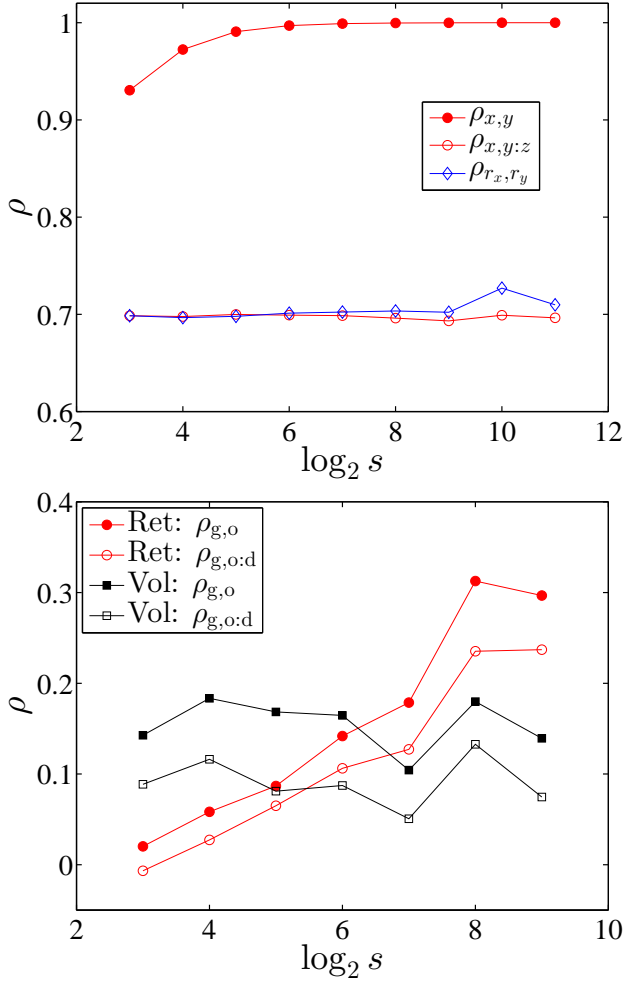


FIG. 2. (color online.) Detrended partial cross-correlation coefficients. (a) Performance of different methods by comparing three cross-correlation coefficients $\rho_{x,y}$, ρ_{r_x,r_y} and $\rho_{x,y;z}$ of the mathematical model in Eq. (8). (b) Estimation and comparison of the cross-correlation levels between the two return time series (o) and two volatility time series (□) of crude oil and gold when including and excluding the influence of the USD index.

have very small Hurst indices $H_{r_x} = 0.1 = H_{r_y} = 0.1$ and their correlation coefficient is $\rho = 0.7$, and the driving FBM force z has a large Hurst index $H_z = 0.95$. Figure 2(a) shows the resulting cross-correlation coefficients at different scales. The DCCA coefficients ρ_{r_x,r_y} between the generated r_x and r_y time series overestimate the true value $\rho = 0.7$. Because the influence of z on r_x and r_y is very strong, the behaviors of x and y are dominated by z , and the cross-correlation coefficient $\rho_{x,y}(s)$ is close to 1 when s is small and approaches 1 when s is large. In contrast, the DPXA coefficients $\rho_{x,y;z}$ are in good agreement with the true value $\rho = 0.7$. Note that the DPXA method better estimates r_x and r_y than the DCCA method, since the ρ_{r_x,r_y} curve deviates more from the horizontal line $\rho = 0.7$ than the $\rho_{x,y;z}$ curve, especially at large scales.

To illustrate the method with an example from finance, we use it to estimate the intrinsic cross-correlation levels between the futures returns and the volatilities of crude oil and gold. It is well-documented that the returns of crude oil and gold futures are correlated [59], and that both commodities are influenced by the USD index [60]. The data samples contain the daily closing prices of gold, crude oil, and the USD index from 4 October 1985 to 31 October 2012. Figure 2(b) shows that both the DCCA and DPXA coefficients of returns exhibit an increasing trend with respect to the scale s , and that the two types of coefficient for the volatilities do not exhibit any evident trend. For both financial variables, Fig. 2(b) shows that

$$\rho_{g,o;d}(s) < \rho_{g,o}(s) \quad (14)$$

for different scales. Although this is similar to the result between ordinary partial correlations and cross-correlations [61], the DPXA coefficients contain more information than the ordinary partial correlations since the former indicate the partial correlations at multiple scales.

III. MULTIFRACTAL DETRENDED PARTIAL CROSS-CORRELATION ANALYSIS

An extension of the DPXA for multifractal time series, notated MF-DPXA, can be easily implemented. When MF-DPXA is implemented with DFA or DMA, we notate it MF-PX-DFA or MF-PX-DMA. The q th order detrended partial cross-correlation is calculated

$$F_{xy;z}(q, s) = \left[\frac{1}{m-1} \sum_{v=1}^m |F_v^2(s)|^{q/2} \right]^{1/q} \quad (15)$$

when $q \neq 0$, and

$$F_{xy;z}(0, s) = \exp \left[\frac{1}{m} \sum_{v=1}^m \ln |F_v(s)| \right]. \quad (16)$$

We then expect the scaling relation

$$F_{xy;z}(q, s) \sim s^{h_{xy;z}(q)}. \quad (17)$$

According to the standard multifractal formalism, the multifractal mass exponent $\tau(q)$ can be used to characterize the multifractal nature, i.e.,

$$\tau_{xy;z}(q) = q h_{xy;z}(q) - D_f, \quad (18)$$

where D_f is the fractal dimension of the geometric support of the multifractal measure [62]. We use $D_f = 1$ for our time series analysis. If the mass exponent $\tau(q)$ is a nonlinear function of q , the signal is multifractal. We use the Legendre transform to obtain the singularity strength function $\alpha(q)$ and the multifractal spectrum $f(\alpha)$ [63]

$$\begin{cases} \alpha_{xy;z}(q) = d\tau_{xy;z}(q)/dq \\ f_{xy;z}(q) = q\alpha_{xy;z}(q) - \tau_{xy;z}(q) \end{cases}. \quad (19)$$

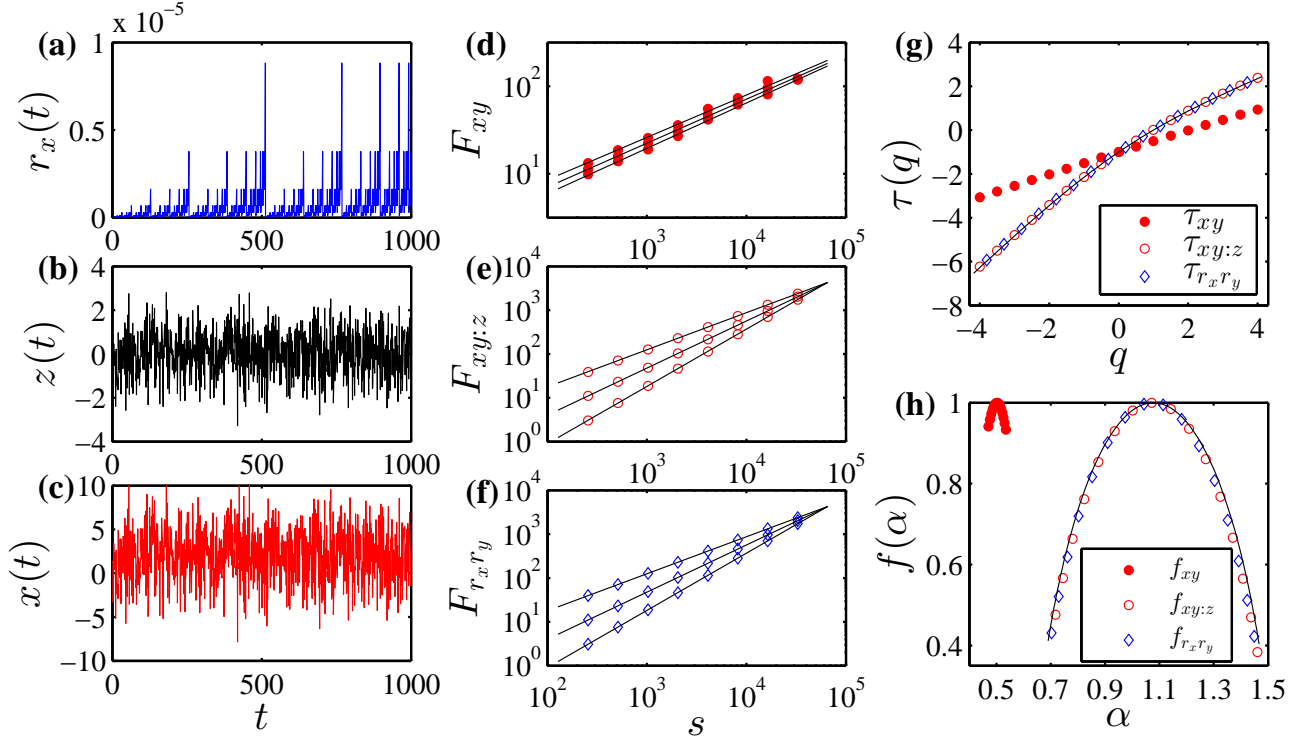


FIG. 3. (color online.) Multifractal detrended partial cross-correlation analysis of two binomial measures contaminated by Gaussian noise with very low signal-to-noise ratio. (a-c) The segments of the binomial signal $r_x(t)$ with $p_x = 0.3$, the Gaussian noise $z(t)$, and the “observed” signal $x(t)$. (d-f) Power-law dependence of the fluctuations $F_{xy}(q, s)$, $F_{xy:z}(q, s)$, $F_{r_x r_y}(q, s)$ on the scale s for $q = -4, 0$ and 4 (top down). The values of $F_{xy:z}$ and $F_{r_x r_y}$ have been multiplied by 10^5 . (g) Multifractal mass exponents $\tau_{xy}(q)$, $\tau_{xy:z}(q)$ and $\tau_{r_x r_y}(q)$, with the theoretical curve $\tau_{r_x r_y}$ shown as a continuous line. (h) Multifractal spectra $f_{xy}(\alpha)$, $f_{xy:z}(\alpha)$, $f_{r_x r_y}(\alpha)$ of the singularity strength α . The continuous curve is the theoretical spectrum $\mathcal{F}_{r_x r_y}(\alpha)$.

To test the performance of MF-DPXA, we construct two binomial measures $\{r_x(t) : t = 1, 2, \dots, 2^k\}$ and $\{r_y(t) : t = 1, 2, \dots, 2^k\}$ from the p -model with known analytic multifractal properties [64], and contaminate them with Gaussian noise. We generate the binomial measure iteratively [38] by using the multiplicative factors $p_x = 0.3$ for r_x and $p_y = 0.4$ for r_y . The contaminated signals are $x = 2 + 3z + r_x$ and $y = 2 + 3z + r_y$. Figures 3(a)–(c) show that the signal-to-noise ratio is of order $O(10^{-6})$. Figures 3(d)–(f) show a power-law dependence between the fluctuation functions and the scale, in which it is hard to distinguish the three curves of F_{xy} . Figure 3(g) shows that for $x(t)$ and $y(t)$, the $\tau_{xy}(q)$ function an approximate straight line and that the corresponding $f_{xy}(\alpha)$ spectrum is very narrow and concentrated around $\alpha = 0.5$. These observations are trivial because $x(t)$ and $y(t)$ are Gaussian noise with the Hurst indices $H_x = H_y = 0.5$, and the multifractal detrended cross-correlation analysis [37] fails to uncover any multifractality. On the contrary, we find that $\tau_{xy:z}(q) \approx \tau_{r_x r_y}(q) \approx \tau_{r_x r_y}(q)$ and $f_{xy:z}(\alpha) \approx f_{r_x r_y}(\alpha) \approx \mathcal{F}_{r_x r_y}(\alpha)$. Thus the MF-DPXA method successfully reveals the intrinsic multifractal nature between $r_x(t)$ and $r_y(t)$ hidden in $x(t)$ and $y(t)$.

IV. SUMMARY

In summary, we have studied the performances of DPXA exponents, DPXA coefficients, and MF-DPXA using bivariate fractional Brownian motions contaminated by a fractional Brownian motion and multifractal binomial measures contaminated by white noise. These mathematical models are appropriate here because their analytical expressions are known. We have demonstrated that the DPXA methods are capable of extracting the intrinsic cross-correlations between two time series when they are influenced by common factors, while the DCCA methods fail.

The methods discussed are intended for multivariate time series analysis, but they can also be generalized to higher dimensions [38, 53, 65, 66]. We can also use lagged cross-correlations in these methods [67, 68]. Although comparing the performances of different methods is always important [69], different variants of a method can produce different outcomes when applied to different systems. For instance, one variant that outperforms other variants under the setting of certain stochastic processes is not necessary the best performing method for other systems [53]. We argue that there are still a lot of open questions for the big family of DFA, DMA, DCCA and

DPXA methods.

ACKNOWLEDGMENTS

This work was partially supported by the National Natural Science Foundation of China under grant no.

11375064, Fundamental Research Funds for the Central Universities, and Shanghai Financial and Securities Professional Committee.

-
- [1] R. A. Antonia and C. W. Van Atta, *J. Fluid Mech.* **67**, 273 (1975).
 - [2] C. Meneveau, K. R. Sreenivasan, P. Kailasnath, and M. S. Fan, *Phys. Rev. A* **41**, 894 (1990).
 - [3] A. N. Kravchenko, D. G. Bullock, and C. W. Boast, *Agron. J.* **92**, 1279 (2000).
 - [4] T. B. Zeleke and B.-C. Si, *Agron. J.* **96**, 1082 (2004).
 - [5] S. Shadkhoo and G. R. Jafari, *Eur. Phys. J. B* **72**, 679 (2009).
 - [6] F. J. Jiménez-Hornero, J. E. Jiménez-Hornero, E. G. de Ravé, and P. Pavón-Domínguez, *Environ. Monit. Assess.* **167**, 675 (2010).
 - [7] D.-C. Lin and A. Sharif, *Chaos* **20**, 023121 (2010).
 - [8] S. Hajian and M. S. Movahed, *Physica A* **389**, 4942 (2010).
 - [9] F. J. Jiménez-Hornero, P. Pavón-Domínguez, E. G. de Rave, and A. B. Ariza-Villaverde, *Atoms. Res.* **99**, 366 (2011).
 - [10] N. Xu, P.-J. Shang, and S. Kamae, *Nonlin. Dyn.* **61**, 207 (2010).
 - [11] X.-J. Zhao, P.-J. Shang, A.-J. Lin, and G. Chen, *Physica A* **390**, 3670 (2011).
 - [12] G. F. Zebende, P. A. da Silva, and A. M. Filho, *Physica A* **390**, 1677 (2011).
 - [13] D.-C. Lin, *Physica A* **387**, 3461 (2008).
 - [14] B. Podobnik, D. Horvatic, A. M. Petersen, and H. E. Stanley, *Proc. Natl. Acad. Sci. U.S.A.* **106**, 22079 (2009).
 - [15] E. L. Siqueira Jr., T. Stošić, L. Bejan, and B. Stošić, *Physica A* **389**, 2739 (2010).
 - [16] Y.-D. Wang, Y. Wei, and C.-F. Wu, *Physica A* **389**, 5468 (2010).
 - [17] L.-Y. He and S.-P. Chen, *Chaos, Solitons & Fractals* **44**, 355 (2011).
 - [18] F. Schmitt, D. Schertzer, S. Lovejoy, and Y. Brunet, *EPL (Europhys. Lett.)* **34**, 195 (1996).
 - [19] G. Xu, R. A. Antonia, and S. Rajagopalan, *EPL (Europhys. Lett.)* **49**, 452 (2000).
 - [20] G. Xu, R. A. Antonia, and S. Rajagopalan, *EPL (Europhys. Lett.)* **79**, 44001 (2007).
 - [21] J. Wang, P.-J. Shang, and W.-J. Ge, *Fractals* **20**, 271 (2012).
 - [22] W. C. Jun, G. Oh, and S. Kim, *Phys. Rev. E* **73**, 066128 (2006).
 - [23] B. Podobnik and H. E. Stanley, *Phys. Rev. Lett.* **100**, 084102 (2008).
 - [24] D. Horvatic, H. E. Stanley, and B. Podobnik, *EPL (Europhys. Lett.)* **94**, 18007 (2011).
 - [25] S. Achard, D. S. Bassett, A. Meyer-Lindenberg, and E. Bullmore, *Phys. Rev. E* **77**, 036104 (2008).
 - [26] S. Arianos and A. Carbone, *J. Stat. Mech.*, P03037 (2009).
 - [27] H. Wendt, A. Scherrer, P. Abry, and S. Achard, in *2009 IEEE International Conference on Acoustics, Speech and Signal Processing* (2009) pp. 2913–2916.
 - [28] T. Qiu, B. Zheng, and G. Chen, *New J. Phys.* **12**, 043057 (2010).
 - [29] T. Qiu, G. Chen, L.-X. Zhong, and X.-W. Lei, *Physica A* **390**, 828 (2011).
 - [30] L. Kristoufek, *Eur. Phys. J. B* **86**, 418 (2013).
 - [31] L. Kristoufek, *Physica A* **406**, 169 (2014).
 - [32] Y. Ying and P.-J. Shang, *Fractals* **22**, 1450007 (2014).
 - [33] L. Kristoufek, *Phys. Rev. E* **91**, 022802 (2015).
 - [34] B. Podobnik, I. Grosse, D. Horvatic, S. Ilic, P. Ch. Ivanov, and H. E. Stanley, *Eur. Phys. J. B* **71**, 243 (2009).
 - [35] G. F. Zebende, *Physica A* **390**, 614 (2011).
 - [36] B. Podobnik, Z.-Q. Jiang, W.-X. Zhou, and H. E. Stanley, *Phys. Rev. E* **84**, 066118 (2011).
 - [37] W.-X. Zhou, *Phys. Rev. E* **77**, 066211 (2008).
 - [38] Z.-Q. Jiang and W.-X. Zhou, *Phys. Rev. E* **84**, 016106 (2011).
 - [39] L. Kristoufek, *EPL (Europhys. Lett.)* **95**, 68001 (2011).
 - [40] D. Y. Kenett, Y. Shapira, and E. Ben-Jacob, *J. Prob. Stat.* **2009**, 249370 (2009).
 - [41] Y. Shapira, D. Kenett, and E. Ben-Jacob, *Eur. Phys. J. B* **72**, 657 (2009).
 - [42] D. Y. Kenett, M. Tumminello, A. Madi, G. Gurgershoren, R. N. Mantegna, and E. Ben-Jacob, *PLoS One* **5**, e15032 (2010).
 - [43] K. Baba, R. Shibata, and M. Sibuya, *Aust. N. Z. J. Stat.* **46**, 657 (2004).
 - [44] Y.-M. Liu, Master's thesis, East China University of Science and Technology (2014), <http://cnki.agrilib.ac.cn/KCMS/detail/detail.aspx?filename=1014170710.nh&dbcode=CMFD&dbname=CMFD2014>.
 - [45] N.-M. Yuan, Z.-T. Fu, H. Zhang, L. Piao, E. Xoplaki, and J. Luterbacher, *Sci. Rep.* **5**, 8143 (2015).
 - [46] C.-K. Peng, S. V. Buldyrev, S. Havlin, M. Simons, H. E. Stanley, and A. L. Goldberger, *Phys. Rev. E* **49**, 1685 (1994).
 - [47] K. Hu, P. C. Ivanov, Z. Chen, P. Carpena, and H. E. Stanley, *Phys. Rev. E* **64**, 011114 (2001).
 - [48] N. Vandewalle and M. Ausloos, *Phys. Rev. E* **58**, 6832 (1998).
 - [49] E. Alessio, A. Carbone, G. Castelli, and V. Frappietro, *Eur. Phys. J. B* **27**, 197 (2002).
 - [50] L. M. Xu, P. C. Ivanov, K. Hu, Z. Chen, A. Carbone, and H. E. Stanley, *Phys. Rev. E* **71**, 051101 (2005).
 - [51] S. Arianos and A. Carbone, *Physica A* **382**, 9 (2007).
 - [52] X.-Y. Qian, G.-F. Gu, and W.-X. Zhou, *Physica A* **390**, 4388 (2011).
 - [53] G.-F. Gu and W.-X. Zhou, *Phys. Rev. E* **82**, 011136 (2010).

- [54] F. Lavancier, A. Philippe, and D. Surgailis, *Statist. Prob. Lett.* **79**, 2415 (2009).
- [55] J.-F. Coeurjolly, P.-O. Amblard, and S. Achard, *Eur. Signal Process. Conf.* **18**, 1567 (2010).
- [56] P.-O. Amblard, J.-F. Coeurjolly, F. Lavancier, and A. Philippe, *Bulletin Soc. Math. France, Séminaires et Congrès* **28**, 65 (2013).
- [57] P. Abry and F. Sellan, *Appl. Comp. Harmonic Anal.* **3**, 377 (1996).
- [58] J. W. Kantelhardt, E. Koscielny-Bunde, H. H. A. Rego, S. Havlin, and A. Bunde, *Physica A* **295**, 441 (2001).
- [59] Y.-J. Zhang and Y.-M. Wei, *Resources Policy* **35**, 168 (2010).
- [60] Y. S. Wang and Y. L. Chueh, *Econometrica* **30**, 792 (2013).
- [61] D. Y. Kenett, X.-Q. Huang, I. Vodenska, S. Havlin, and H. E. Stanley, *Quant. Finance* **15**, 569 (2015).
- [62] J. W. Kantelhardt, S. A. Zschiegner, E. Koscielny-Bunde, S. Havlin, A. Bunde, and H. E. Stanley, *Physica A* **316**, 87 (2002).
- [63] T. C. Halsey, M. H. Jensen, L. P. Kadanoff, I. Procaccia, and B. I. Shraiman, *Phys. Rev. A* **33**, 1141 (1986).
- [64] C. Meneveau and K. R. Sreenivasan, *Phys. Rev. Lett.* **59**, 1424 (1987).
- [65] G.-F. Gu and W.-X. Zhou, *Phys. Rev. E* **74**, 061104 (2006).
- [66] A. Carbone, *Phys. Rev. E* **76**, 056703 (2007).
- [67] B. Podobnik, D. Wang, D. Horvatic, I. Grosse, and H. E. Stanley, *EPL (Europhys. Lett.)* **90**, 68001 (2010).
- [68] C.-H. Shen, *Phys. Lett. A* **379**, 680 (2015).
- [69] Y.-H. Shao, G.-F. Gu, Z.-Q. Jiang, W.-X. Zhou, and D. Sornette, *Sci. Rep.* **2**, 835 (2012).